Pergamon

Int. J. Heat Mass Transfer. Vol. 37, No. 18, pp. 2925–2933, 1994

0017–9310/94 $7.00+0.00

0017–9310(94)E0098–F

Eddy break-up model and fractal theory: comparisons with experiments

F. NICOLLEAU and J. MATHIEU

Ecole Centrale de Lyon/Université Claude Bernard—Lyon 1
Laboratoire de Mécanique des Fluides et d'Acoustique, URA CNRS 263, ECL, B.P. 163,
69131 Ecully Cedex, France

(*Received* 22 *February* 1993 *and in final form* 18 *March* 1994)

Abstract—This paper deals with predictive methods of the combustion rates in the case of premixed mixtures. Comparisons are made between two of these predictive methods. The first approach is based on a standard eddy break-up (EBU) model supplemented by a condition on the chemical composition of the mixture. The reaction can develop within a fixed range of richness. The second method uses the concept of fractal surfaces. Moreover a spectral analysis allows us to introduce the role of the small turbulent structures embedded in the preheat zone. By means of the concept of fractal surfaces the real area of the flame surface can be predicted starting from its mean value and from L (integral length scale), u' and η_K (Kolmogorov length scale). The location of the flame is deduced from the standard EBU model previously referred to. u' and $\langle\varepsilon\rangle$ are also known along the mean flame surface. The area of the real indented surface can be inferred. The combustion rate can be deduced by associating the area of the flame front with a convenient flame speed accounting for the role of the small structures embedded in the preheat zone. The results found by the two methods do not depart from each other by more than 10%

1. INTRODUCTION

Among computing methods dealing with combustion, methods based on p.d.f. (Dopazo [1]) and methods based on flame-front description are the most popular (Williams [2]). Viewed in its entirety the approach based on p.d.f. could find a wide field of application because it does not require an accurate description of the phenomenon as such. The concept of flame assumes the existence of a threefold mechanism with chemical reaction, advection and heat transfer [3]. This approach was proposed by Barrère [4], Delamare *et al.* [5] and Peters [6], and a modern analysis has been developed by Poinsot *et al.* [7, 8]. When a flame is immersed in a turbulent field this calls into question the possibility of imagining a front which becomes a convoluted surface with a sudden change of scalar quantities such as temperature or concentration of species. The concept of laminar flame is well stated, but to what extend this concept may be enlarged to higher levels of turbulence with sharper indentations of the surface is still an open question. A spectral description of this problem displays how the smallest turbulent structures may—or may not—be immersed in the flame front [3]. When the thickness of the flame is smaller than the Kolmogorov length scale then the flame is acted upon by the turbulent motion which behaves as though it were an external stimulator. In contrast, when the thickness of the flame is larger than the Kolmogorov length scale then the flame is invaded by a fine-grained turbulence which firstly alters the preheat zone. We tentatively enlarge the physical concept of the laminar flame front, which is clearly associated with well-identified mechanisms, to less restrictive situations by introducing credible assumptions.

To a large extent, for flames identified with zones of high gradients of both concentration and temperature, the development of the flame could be supported by all the approaches concerned with the evolution of any convoluted surface in two or three dimensions (cf. Darabiha *et al.* [9], Maistret *et al.* [10], Candel *et al.* [11]). That leads us to introduce a fractal scheme for a better understanding of the development of the front. This concept has already been investigated by several researchers: Peters [6], Gouldin [12], Mantzaras [13], Santavicca [14]. This effort will also be associated with an evaluation of the 'turbulent speed of the flame'—particularly due to increasing heat exchange within the preheat zone. To do this the chemical time is supposed to be constant, an assumption which is mainly justify by the success of the method based on it (cf. Borghi [15] and Peters and Barrère, private communication). Finally an assessment of the predictive methods will be proposed for the case of moderate and high values of the Damköhler number ($Da \geqslant 1$). Other attempts to implement the fractal concept in modelling exist (Gouldin *et al.* [16, 17]) and an approach using multifractal theory was carried out by Meneveau *et al.* [18].

2. THE FRACTAL SCHEME

Starting from the concept of internal intermittence the turbulent flow appears to be strongly inhomogeneous at a given time: the higher the Reynolds

NOMENCLATURE

A	surface area
D'	fractal dimension of a surface
D	fractal dimension of a volume
$E(k)$	energy spectrum
EBU	eddy break-up
k	wave number
L	integral length scale
Pr	Prandtl number
r	size of a structure
s	arc length
t	time
u'	root mean square value of the fluctuation of the turbulent velocity
u_l	laminar flame speed
u_l^*	thick flame speed
v_K	Kolmogorov velocity scale
W_B	local burning rate
x, y, z	spatial coordinates
Y_i	mass fraction for the species i
Y_{Mi}	maximum value for Y_i in the EBU model.

Greek symbols

α	thermal diffusion coefficient
α_T	turbulent thermal diffusion coefficient
δ_l	laminar flame thickness
δ_l^*	thickness of thick flame
ε	dissipation rate
η_K	Kolmogorov length scale
μ_2	$D'-2$
ν	kinematic viscosity
ν_T	spectral turbulent viscosity
ρ	mass density of the reactant
ρ^*	mass density of the fresh mixture
τ_{ch}	chemical time
$\dot{\omega}_i$	source term for the species i.

Other symbols

$\bar{f}$	mean value
$\tilde{f}$	Favre mean value.

number, the less extended the region occupied by the small structures responsible for the dissipation. Internal intermittence, which generates high-velocity-gradient zones, acts also on immersed surfaces and strains them and locally generates strong indentations. Among all existing surfaces the frontier of the flow is the easiest to identify: it is subjected to the same sort of stimulations as any of them. Therefore a fundamental theory which explains intermittence prepares the ground for detailed explorations of the history of any immersed surface. That explains recent applications of multifractal and fractal theories to predictive methods available for diffusion flames. For instance, Meneveau *et al.* [18] use this approach to refine quenching criteria.

A growing interest for multifractal theories has been developed in the last years by Sreenivasan *et al.* [19, 20], Meneveau *et al.* [21, 22], Gagne [23], Vassilicos and Hunt [24]. An overview of this topic has also been presented by Nicolleau *et al.* [25].

Multifractal theory can be introduced in several ways, the most physical is based on an internal invariance of the Navier–Stokes equations. As far as motions of fluid elements depend on inertial forces only, this invariance is verified. Recent research shows that, by using the technique of fractals, certain properties relating to the self-similarity and the space filling of interfaces can be studied in more detail than by traditional methods of spectra and auto correlations.

We can suppose a possible identification of the turbulent structures through the relation $\Delta u_r \sim r^h$, where Δu is the modulus of the difference of velocity between two points of a doublet with a size r, and h is the scale exponent. Examining a realization of the velocity field, we can identify the region where the scale exponent has a certain value. This assessment leads us to the definition of a fractal set corresponding to this value of h. This power law may be considered as a generalization of the one encountered in a swirling motion.

Each statistical moment of u is associated with a fractal set S. Thanks to the multifractal theory it may be written:

$$\frac{\langle u^p(r)\rangle}{u'^p} \sim \left(\frac{r}{L}\right)^{C(p)}. \tag{1}$$

$C(p)$ is related to the fractal dimension of S, and r and L stand for the distance of a couple of points (doublet) and for an integral length scale respectively.

In other words $\langle u^p(r)\rangle$ represents the contribution to the statistical moment $\langle u^p\rangle$ of doublets when r is the spatial distance between the two points. $C(p)$ may be determined from experimental data (Gagne [23]). A relation similar to (1) is available for ε:

$$\frac{\langle \varepsilon^p(r)\rangle}{\langle \varepsilon\rangle^p} \sim \left(\frac{r}{L}\right)^{\mu(p)}$$

where $\mu(p)$ is the equivalent of $C(p)$ for the statistical moments of the dissipation rate ε. This model has direct consequences on the development of surfaces immersed in turbulent fields. An iso-scalar surface behaves as a fractal surface whose fractal dimension D' is related to the multifractal model according to the relation

$$(D'-2) = \tfrac{1}{3} + \mu(\tfrac{1}{3}) \tag{2}$$

where $\mu(\frac{1}{3})$ is a characteristic parameter of the multifractal theory.

The evaluation of the area of the surface depends on the scale L—or η_i—used to describe the geometry. It finally yields

$$A = A_0 \left(\frac{L}{\eta_i}\right)^{D'-2} \tag{3}$$

We will set $D'-2 = \mu_2$. For usual surface $\mu_2 = 0$, large values of μ_2 ($0 < \mu_2 < 1$) correspond to strongly indented surfaces.

We can also introduce the multifractal theory by means of a random approach. In this case, in the relation $\Delta u_r \sim r^h$, h is assumed to be a random variable. Convenient hypotheses on the probability density function of h lead to the same results.

3. COMBUSTION PROCESSES

We briefly recall and extend concepts used in the case of premixed flames.

3.1. *Fundamental parameters used for the description of flames developing in a turbulent medium*

Usually reference is made to parameters related to both the flow and the flame.

3.1.1. *Flow parameters.* With a view to industrial applications reference will be preferentially made to the k–$\bar{\varepsilon}$ model, which is still the most popular. The most usual parameters are listed below:

- the root mean square of the velocity fluctuation u'
- the mean dissipation rate $\bar{\varepsilon}$
- the integral length scale L
- the Kolmogorov length scale η_K
- the mean velocity $\bar{U}_i$, and the mean pressure $\bar{P}$.

In as much as assumptions are often made, these quantities may appear to be linked to each other. For instance, when a spectral equilibrium is assumed, the integral scale L and the dissipation rate $\bar{\varepsilon}$ are connected with each other through the Reynolds number.

3.1.2. *Flame parameters.* For the flame, reference is made to its speed (laminar flame speed u_l) and to its thickness δ_l. The chemical reaction is associated to a heat release Q. The rate of Q introduces a chemical characteristic time.

From the global parameters previously mentioned, several combustion patterns may be defined. Their identification can be made by means of diagrams whose state of refinement increases in time. In first attempts the characterization of the combustion process was only related to quantities defined in the physical space such as u' and L. The diagrams proposed by Barrère [4], Dclamare *et al.* [5] and later by Peters [6] (see Fig. 1) use these types of global quantities. The capability of spectral methods to describe more carefully the combustion regimes was introduced by Mathieu *et al.* [3]. Based on a similar approach and using two-dimensional direct simulation Poinsot *et al.*

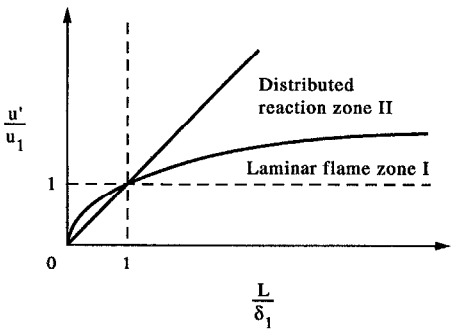

Fig. 1. Barrère–Borghi–Peters diagram.

[7, 8] predicted quenching processes. These authors emphasized the dominant role of the intermediate (rather than the small-scale) structures on the quenching of flames. This finding may also be confirmed by introducing the concept of cumulative strain (a dimensionless parameter) (Nicolleau *et al.* [26]). The flame is acted upon by the intense stretching of the smallest structures during a very short time. Due to the largest structures, the flame is subjected to a low straining process but over a long period. One can presume that the combined role of both strain and time is maximum where intermediate structures are concerned. These findings display the role of more refined approaches, and confirm the role of spectral analysis in specifying the influence of turbulence on flames.

3.2. *The concept of flame front*

The flame front is roughly identified as a discontinuity surface of high gradient for parameters such as concentration of species, temperatures, etc. This point of view permits a gradual approach of the turbulent flame. First we begin with an identification of the motion of the surface and, second, we evaluate the influence of turbulence on the flame speed.

The concept of laminar flame speed is based on firm theory (Kuo [27] and Williams [28]), even though some mathematical aspects of this problem are still open; among them being the uniqueness of the solution. In this paper we accept without restriction the concept of laminar flames having a characteristic speed.

Extensions of the concept of laminar flame to turbulent flows will also be accepted (see Fichot *et al.* [29]). If the thickness of the flame is small enough, turbulence can be thought of as an external stimulator. The flame front is distorted but the preheat and chemical zones are too thin to be invaded by fine-grained structures.

As the Reynolds number increases, the Kolmogorov length-scale decreases and finally the smallest structures penetrate the preheat zone (not the chemical zone which is thinner). The concept of a laminar flame cannot be kept as such: it should be enlarged.

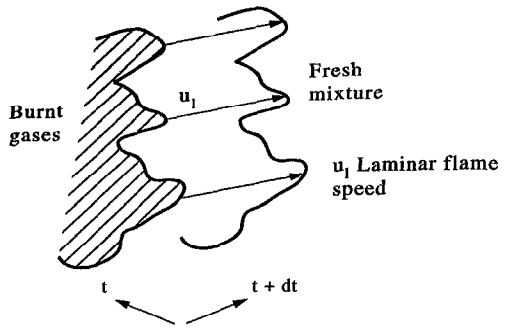

Fig. 2. The burning process.

When the chemical zone is invaded the new situation is out of the scope of this paper by reason of the possible alteration of the chemical characteristic time.

A unique parameter is meaningful, namely the burning rate, which represents the mass rate of burnt gases. In this case, combustion is considered as a whole and the definition is consistent whatever the sort of flame under consideration.

When the concept of flame front or flame speed is locally maintained another point of view may be explored. The flame propagation being supposed normal to the flame front, we can assume the burning rate to be locally defined by (cf. Damköhler [30], Dumont *et al.* [31])

$$W_B = \rho u_l A \tag{4}$$

where W_B stands for the burning rate, ρ is the density of the reactant, u_l is the laminar speed of the flame and A stands for the surface area of the flame front.

A sketch of the burning process related to this definition is presented in Fig. 2.

In order to permit comparisons, the concept of turbulent flame speed is improperly used. In fact this flame speed may be considered as the velocity of a fictitious plane flame with a surface equal to A_0 and giving the same burning rate. In other words, we have

$$u_T = \left(\frac{W_B}{\rho A_0}\right). \tag{5}$$

4. AN APPLICATION OF FRACTAL THEORY

Referring to relation (3) the flame area can be estimated. That leads to a relation deduced from equation (4):

$$W_B = \rho u_l A_0 \left(\frac{L}{\eta_i}\right)^{\mu_2}. \tag{6}$$

We recall that $\mu_2 = D' - 2$ measures how the geometrical shape of the reactive surface departs from a two-dimensional geometry. Santavica *et al.* [14] use formula (6) with D' varying from 2 to 2.35 according to the turbulence intensity u' and obtain good agreement with experiments for combustion ignited near the spark. This relation seems to be adequate for at least specific situations, for instance, when the turbulence intensity is small or in the first step of the ignition process as referred to in ref. [14].

4.1. *The case of corrugated flames*

The burning rate can easily be introduced in the case of wrinkled flames. This corresponds to zone I of the standard combustion diagram. In this domain the cut-off value η_i is taken equal to η_K: consequently the properties of the turbulent field determine this cut-off value. It is easily seen that

$$W_B = \rho u_l A_0 \left(\frac{L}{\eta_K}\right)^{\mu_2}. \tag{7}$$

The classical value of D' ($D' = 2.36$, cf. refs. [13] and [20]) is then inserted in the previous relation, yielding

$$W_B = \rho u_l A_0 \left(\frac{L}{\eta_K}\right)^{0.36}. \tag{8}$$

The dependence of L/η_K on the Reynolds number can be written as

$$\frac{u_T}{u_l} \sim (Re^{3/4})^{0.36} \tag{9}$$

and we find that

$$\frac{u_T}{u_l} \sim \left(\frac{u'}{u_l}\right)^{0.27} \left(\frac{L}{\delta_l}\right)^{0.27} Pr^{0.27}. \tag{10}$$

We have the same exponent for u' and L.

During the burning process the variations of the integral scale L are supposed to be small compared with those of u'. Finally that yields

$$\frac{u_T}{u_l} \sim \left(\frac{u'}{u_l}\right)^{0.27}. \tag{11}$$

Even though this result is supported by ref. [14] it may be considered as rather an unexpected issue. Usually in the literature u_T is related to u' by a power law (Peters [6], Bradley [32], Bray [33], e.g. $u_T \sim u'^{\alpha}$ with $0.5 < \alpha < 1$). In the next section the action of the turbulence on the reactive fronts will be accounted for in order to improve relation (11).

4.2. *Alterations of both the speed of the flame and the flame thickness*

An analysis of the combustion process near zone II in the diagram is more complex and requires additional comments.

First of all, the speed of the flame is altered. With laminar flames, this speed is linked both to the thermal diffusion coefficient α and to the chemical time τ_{ch}. Finally the flame process results from a delicate balance between three mechanisms: diffusion, advection, and chemical reaction. Each of them has a characteristic time, so that the presumed equilibrium estab-

lished in the flame exists when these three characteristic times have the same order of magnitude, that is:

$$\tau_{ch} \sim \frac{\delta_l}{u_l} \sim \frac{\delta_l^2}{\alpha} \quad u_l = \sqrt{\frac{\alpha}{\tau_{ch}}} = \frac{\delta_l}{\tau_{ch}}. \tag{12}$$

When the turbulent structures penetrate the preheat zone, diffusion processes are enhanced and the previous equilibrium must be re-examined. However, turbulent structures can invade the preheat zone without penetrating the chemical zone. Hence the characteristic chemical time linked to the chemical zone is supposed to be unchanged—whatever the surrounding flow, laminar or turbulent. This situation is assumed to be valid for a limited range of the Damköhler number ($Da \geqslant 1$). Accordingly a characteristic length playing the role of a flame thickness δ_l^* may be introduced and also a flame speed u_l^*. The presumed reaction zone behaves much like a laminar flame except for the two quantities δ_l^* and u_l^*, which have to be re-evaluated in order to account for a fine-grained turbulence within the preheat zone. This leads to a re-evaluation of the diffusion process which becomes the consequence of both molecular and turbulence effects through the relation:

$$\alpha^* = \alpha + \alpha_T. \tag{13}$$

In the case of a laminar and turbulent Prandtl number equal to unity we have:

$$\nu_T = \alpha_T. \tag{14}$$

It is known that for usual chemical species present in the reactive zone this dimensionless number is different from one. This situation can create specific mechanisms which locally come into play in the case of a curved reactive zone.

Presumably the role of small turbulent structures immersed in the preheat zone may be accounted for by means of a diffusion coefficient based on both length and velocity scales. For such an evaluation a local distribution of the turbulent kinetic energy must be postulated for the spectral range corresponding to structures immersed in the preheat zone. Figure 3 describes the three possible combustion–turbulence interaction modes.

Kolmogorov's spectrum seems to be a simple but questionable approximation when the integration is made over a domain extended up to $1/\eta_K$. This gives

$$\nu_T = c_2 \int_{1/\delta_l^*}^{1/\eta_K} \left(\frac{E(k)}{k^3}\right)^{\frac{1}{2}} dk \quad \text{with } c_2 \sim 1. \tag{15}$$

The local length scale has been chosen equal to $1/k$.

For the sake of accuracy in this domain of integration Pao's spectrum

$$E(k) = C\langle\varepsilon\rangle^{2/3} k^{-5/3} \exp\left(-\frac{3C}{2}(k\eta)^{4/3}\right)$$

would be a more convenient approximation. We tentatively introduce it without significantly altering the results. Finally, Kolmogorov's spectrum, $E(k) = c_1\langle\varepsilon\rangle^{2/3}k^{-5/3}$ with $c_1 \sim 1.5$, has been used. This formulation yields simple final expressions which display the role of all the parameters u', L, D', etc. ν_T is deduced from an integration made over the domain δ_l^* to η_K.

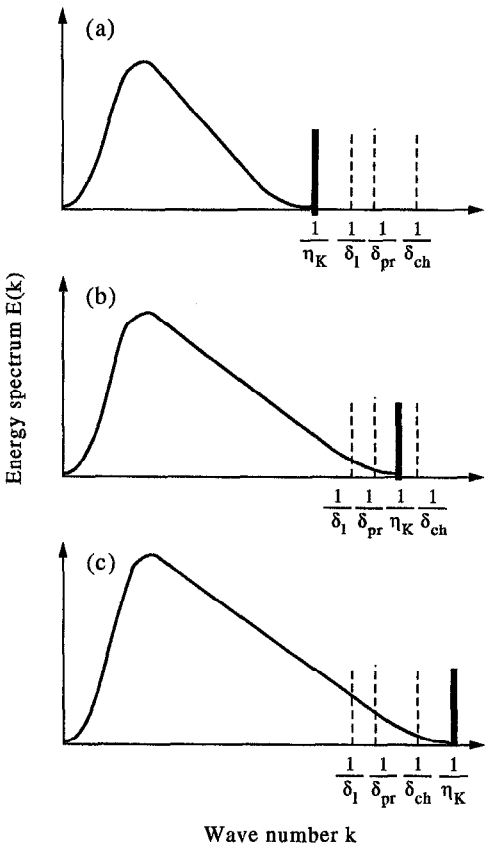

Fig. 3. Mathieu's diagram. This spectral approach emphasizes three types of flame–turbulence interaction: A corresponds to the laminar flame, B to the interaction considered in Section 4.2, C describes a case where chemical zone is invaded with turbulent structures, this case is out of our scope.

We obtain

$$\nu_T = c_1 c_2 \langle\varepsilon\rangle^{\frac{1}{3}} \int_{1/\delta_l^*}^{1/\eta_K} \left(\frac{k^{-5/3}}{k^3}\right)^{1/2} dk \tag{16}$$

and after some computations this gives

$$\frac{\nu_T}{\frac{3}{4}c_1 c_2} = \nu\left[\left(\frac{\delta_l^*}{\eta_K}\right)^{4/3} - 1\right] \quad \text{with } \tfrac{3}{4}c_1 c_2 \sim 1 \tag{17}$$

and finally:

$$\frac{\nu_T}{\nu} + 1 = \frac{\alpha_T}{\alpha} + 1 = \left[\frac{\delta_l^*}{\eta_K}\right]^{4/3}. \tag{18}$$

Returning to the expression for u_l^* (12) then becomes

$$u_l^{*2} = \frac{\alpha^*}{\tau_{ch}} = (\alpha+\alpha_T)\frac{1}{\tau_{ch}} = \frac{\alpha}{\tau_{ch}}\left(1+\frac{\alpha_T}{\alpha}\right) \quad (19)$$

$$u_l^{*2} = u_l^2\left(\frac{\delta_l^*}{\eta_K}\right)^{4/3} \quad (20)$$

and hence

$$u_l^* = u_l\left(\frac{\delta_l^*}{\eta_K}\right)^{2/3}. \quad (21)$$

Compared with equation (12) it yields

$$u_l^* = \left(\frac{\delta_l^*}{\tau_{ch}}\right) = \left(\frac{\delta_l}{\tau_{ch}}\right)\left(\frac{\delta_l^*}{\eta_K}\right)^{2/3} \quad (22)$$

and hence

$$\frac{u_l^*}{u_l} = \left(\frac{\delta_l^*}{\eta_K}\right)^{2/3}. \quad (23)$$

It may also be shown that

$$1 = \left(\frac{\delta_l}{\eta_K}\right)\left(\frac{\eta_K}{\delta_l^*}\right)^{2/3} \Rightarrow \left(\frac{\delta_l^*}{\eta_K}\right) = \left(\frac{\delta_l}{\eta_K}\right)^3 \quad (24)$$

and consequently one finds

$$\frac{\delta_l^*}{\eta_K} = \left(\frac{\delta_l}{\eta_K}\right)^3. \quad (25)$$

The turbulent flame speed u_l^* is finally shown to be essentially dependent on characteristics related to laminar properties as written here:

$$u_l^* = u_l\left(\frac{\delta_l}{\eta_K}\right)^2. \quad (26)$$

Relations (25) and (26) are valid when δ_l is larger than η_K ($\delta_l > \eta_K$).

4.3. *An estimation of the combustion rate*

Due to the growing thickness of the flame the fractal process has to be applied up to δ_l^*, not up to η_K as previously made. From equations (4) and (26) one finds

$$W_B = \rho u_l\left(\frac{\delta_l}{\eta_K}\right)^2\left(\frac{L}{\delta_l^*}\right)^{\mu_2} A_0 = \rho u_l A_0\left(\frac{\delta_l}{\eta_K}\right)^2\left(\frac{L}{\delta_l}\frac{\delta_l}{\eta_K}\frac{\eta_K}{\delta_l^*}\right)^{\mu_2} \quad (27)$$

and hence

$$W_B = \rho u_l A_0\left(\frac{\delta_l}{\eta_K}\right)^2\left(\frac{L}{\delta_l}\right)^{\mu_2}\left(\frac{\delta_l}{\eta_K}\right)^{\mu_2}\left(\frac{\delta_l}{\eta_K}\right)^{-3\mu_2}. \quad (28)$$

After some rearrangements this yields

$$W_B = \rho u_l A_0\left(\frac{\delta_l}{\eta_K}\right)^{2(1-\mu_2)}\left(\frac{L}{\delta_l}\right)^{\mu_2}. \quad (29)$$

In this equation W_B appears to be dependent on both laminar parameters δ_l and u_l and turbulent parameters η_K, L and μ_2.

A more convenient form can also be inferred. For practical application, reference should preferentially be made to quantities directly deduced from the k–$\bar{\varepsilon}$ model, that is L and u'. In the case of a spectral equilibrium, we recall that

$$\eta_K \sim (\bar{\varepsilon})^{-1/4}\nu^{3/4} \quad \text{and} \quad \bar{\varepsilon} \sim u'^3/L.$$

Hence we have

$$W_B = W_0\left(\frac{\delta_l u_l}{\nu}\right)^{(3(1-\mu_2))/2}\left(\frac{u'}{u_l}\right)^{(3(1-\mu_2))/2}\left(\frac{L}{\delta_l}\right)^{(3\mu_2-1)/2}. \quad (30)$$

W_0 stands for $W_0 = \rho\mu_l A_0$ which is the burning rate in the case of laminar flows.

When inserting the classical value of μ_2 ($\mu_2 = 0.36$) in equation (30) it is found that

$$\frac{W_B}{W_0} = \left(\frac{\delta_l u_l}{\nu}\right)^{0.96}\left(\frac{u'}{u_l}\right)^{0.96}\left(\frac{L}{\delta_l}\right)^{0.04}. \quad (31)$$

Equation (31) displays a weak dependence between W_B and L/δ_l. At present, the role of this last parameter is poorly known: referring to equation (30) variation of W_B with u'/u_l and L/δ_l strongly depends on the fractal dimension of the flame front. The quasi-proportionality of W_B with u' only exists for the usual values of D' and μ_2 ($D' = 2.36$, $\mu_2 = 0.36$). These values have been found in many situations but we are not yet sure whether they can be extrapolated to all the usual situations (for instance in the wall region). Due to the fact that the sum of the two exponents is equal to one, balanced effects exists between u'/u_l and L/δ_l. If W_B strongly depends on u'/u_l then it weakly depends on L/δ_l. In the case of $D' = 2.33$ and $\mu_2 = 0.33$ we find that W_B is proportional to u' and independent of L. It is worth noting, by contrast, that with $D' = 3$, W_B is only dependent on L/δ_l.

With $\mu_2 = 0.36$ the dependence of W_B on L/δ_l can be neglected: moreover we can set $\delta_l U_l/\nu \sim 1$ (Prandtl number equal to 1) which leads to

$$\frac{W_B}{W_0} = \left(\frac{u'}{u_l}\right)^{0.96}. \quad (32)$$

In this case, the burning rate appears to be quasi-proportional to u'. This result is in agreement with experimental data given by Bradley [32], Peters [6], Bray [33], Kuznetsov and Sabel'nikov [34]. This dependence is very clear if a limited number of intermediate species intervenes in the reaction (as is the case with a hydrogen–oxygen premixture). For high values of u' the previous assumptions are no longer valid: the experimental curve falls below the previous prediction. With other models that attempt to evaluate a possible meeting between two chemical species, such as the EBU model, this proportionality is not evident. A characteristic time intervenes which also displays a strong dependence of the process on u'. However, other quantities related to the concentration of species that obey coupled partial differential equa-

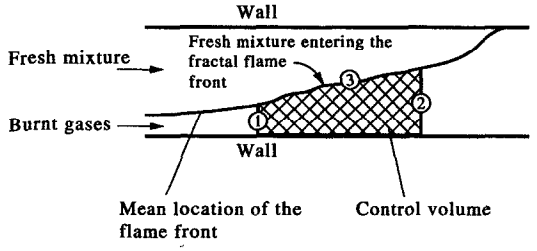

Fig. 4. Moreau experiment: the budget of burnt gases between 1 and 2 is compared with the burning rate calculated at 3.

tions interfere. Finally the dependence is far more difficult to predict.

A global relation may be proposed in the form:

$$\frac{W_B}{W_0} = \int \left(\frac{u'}{u_l}\right)^{0.96} \left(\frac{L}{\delta_l}\right)^{0.04} \frac{dA}{A_0}. \tag{33}$$

5. COMPARISONS WITH NUMERICAL CODES

5.1. *The two patterns of flow under consideration*

The code NATUR has been used to predict the development of combustion. It has been applied to two typical cases. This code is founded on both a k–$\bar{\varepsilon}$ model for turbulence and a standard EBU model supplemented by a condition for the chemical composition of the mixture for combustion. This code has been developed, improved and implemented by Brun [35] and Buffat [36] at the Fluid Mechanics Laboratory of the Ecole Centrale de Lyon. Two reference cases have also been predicted by these authors and compared with experimental results:

- a flame investigated by Moreau
- a flame established behind a step holder.

These flows are sketched in Figs. 4 and 5.

5.2. *Validation of the theoretical relation*

The NATUR code has been validated, in particular in the case of Moreau's flame. We compare our results with those delivered by this code. For this comparison, we refer to budgets of burnt gases at two stations respectively, as described in Fig. 4. The high values of the ratio v_K/u_l deduced from numerical results validate the assumptions made in the case of a thick flame. Wall regions are taken to be outside the control volume in a geometrical domain referred to in Figs. 4 and 5.

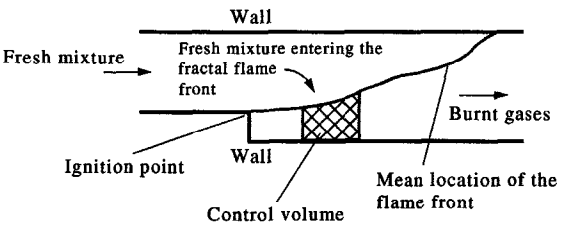

Fig. 5. Flame established behind a step holder: the computation carried out in the control volume is described in Fig. 4.

Table 1

Without term $(L/\delta_l)^{0.04}$	$d = 1.52$ kg s^{-1}	13%
$\delta_l = 0.001$ m	$d = 1.68$ kg s^{-1}	4%
$\delta_l = 0.0001$ m	$d = 1.84$ kg s^{-1}	5%

5.2.1. *Moreau's flame.* From the code the variation of the flow rate is equal to $d = 1.74$ kg s^{-1}. Typical data are: $\rho^* = 0.569$ kg m^{-3} is the density of the fresh mixture, $u_l = 0.9$ m s^{-1} is the laminar flame speed. The thickness of the laminar flame is poorly known: for the sake of simplification the term $(L/\delta_l)^{0.04}$ will be neglected and two extreme cases arbitrarily chosen ($\delta_l = 0.001$ m and $\delta_l = 0.0001$ m).

Results are presented in Table 1 and Fig. 6. The most representative quantity is the error evaluated by reference to the values delivered by the numerical code.

5.2.2. *Backward facing step experiment.* Comparisons have been made in the case of a flame established behind a backward-facing step. In this case the flow-rate variation predicted by the code is $d = 0.65$ kg s^{-1}. The data are: $\rho^* = 0.65$ kg m^{-3} density of the fresh gases, $u_l = 0.9$ m s^{-1} laminar speed of the flame.

The results are presented in Table 2 and Fig. 7. The errors are still evaluated by reference to the results of the code.

5.3. *Applications to numerical codes*

These first two comparisons being encouraging, we return to the fractal theory in order to display the consistency of these results.

In the code NATUR the source term is modelled by

$$\tilde{\dot{\omega}}_i = \frac{a}{\tau}(\tilde{Y}_i - \tilde{Y}_M)\tilde{Y}_i \tag{34}$$

with

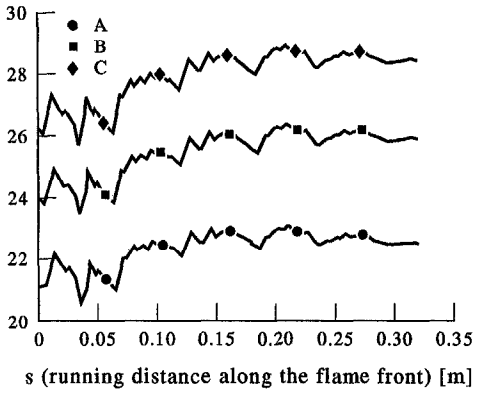

Fig. 6. Flame investigated by Moreau. A: $(u'/u_l)^{0.96}$ vs s (in m); B: $(u'/u_l)^{0.96}(L/\delta_l)^{0.04}$ with $\delta_l = 1$ mm vs s (in m); C: $(u'/u_l)^{0.96}(L/\delta_l)^{0.04}$ with $\delta_l = 0.1$ mm vs s (in m).

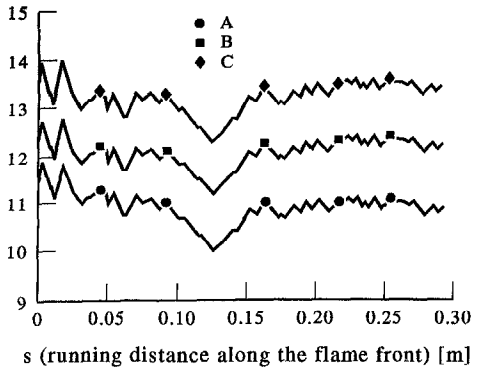

Fig. 7. Flame established behind a step holder. A: $(u'/u_l)^{0.96}$ vs s (in m); B: $(u'/u_l)^{0.96}(L/\delta_l)^{0.04}$ with $\delta_l = 1$ mm vs s (in m); C: $(u'/u_l)^{0.96}(L/\delta_l)^{0.04}$ with $\delta_l = 0.1$ mm vs s (in m).

$$\frac{a}{\tau} = C_{EBU}\frac{\tilde{\varepsilon}}{k}. \tag{35}$$

C_{EBU} and a are two constants.

The characteristic time introduced in the combustion process is in fact the time of decay of turbulence. Therefore it accounts for the cascade process which develops in the inertial range.

5.3.1. *A characteristic time linked to fractal theory.* The characteristic time for the combustion may be defined as follows:

$$t_c = \frac{m_0}{W_B} \tag{36}$$

where m_0 is the mass of fluid inside the control volume and W_B is the burning rate. A possible choice for m_0 is $\rho A_0 L$: L is still the integral scale.

In the case of a thick flame this yields

$$t_c = \left(\frac{\delta_l}{u_l}\right)^{(3\mu_2-1)/2}\left(\frac{L}{u'}\right)^{3(1-\mu_2)/4} \tag{37}$$

and replacing μ_2 by its value 0.36 yields

$$t_c = \left(\frac{\delta_l}{u_l}\right)^{0.04}\left(\frac{L}{u'}\right)^{0.96}. \tag{38}$$

No coupled terms appear and the characteristic turbulent time L/u' becomes predominant.

5.3.2. *Application to the code.* Referring to relation (35), we replace the characteristic time by the one deduced from fractal theory. In the frame of an EBU theory this change of characteristic time is equivalent to writing

Table 2

Without term $(L/\delta_l)^{0.04}$	$d = 0.62$ kg s^{-1}	6%
$\delta_l = 0.001$ m	$d = 0.68$ kg s^{-1}	4.5%
$\delta_l = 0.0001$ m	$d = 0.75$ kg s^{-1}	15%

$$C_{EBU}(\text{fractal}) = C_{EBU}\left(\frac{k}{\tilde{\varepsilon}}\right)^{-0.04}\left(\frac{\delta_l}{u_l}\right)^{-0.04}.$$

The two characteristic times do not appear very different from each other, a fact which can be explained by the leading role played by the cascade process in the two approaches.

6. CONCLUSION

We have compared results given by a standard EBU model supplemented by a condition for the chemical composition of the mixture with results derived from an approach based on the local behaviour of reaction zones. The flame may be considered as being acted upon by external 'stimulators' such as turbulence when the flame thickness δ_l is smaller than the Kolmogorov length scale η_K. We tentatively introduce the concept of a thick reaction zone which corresponds to a penetration of turbulence into the flame zone. The area of the flame front scales on the flame thickness. An evaluation of the real area of the flame front is made possible by means of fractal theory. The integral scale and the level of turbulence are assumed to be known at each point of the localized flame front. A new flame speed is introduced which accounts for the role of a fine-grained turbulence that invades the preheat zone. With these two data, that is, the real area of the flame front and the flame speed, the burning rate can be deduced. The burning rates deduced from the two methods do not depart from each other by more than about 10%.

This good agreement is not so surprising if we make reference to the physical background of these two methods. The chemical reaction that is initiated by the contact of a hot point with the fresh mixture is controlled by the cascade process. In the EBU model the main assumption refers to the source term with the introduction of a chemical time. This eventually becomes a mechanical time [i.e. the time of decay of the turbulence: expressions (34) and (35)]. This approximation is possible only if the chemical time is very small compared with the characteristic time of the turbulent cascade process. In other words the chemical reaction is driven by a dynamic process which is only related to the non-linear interactions which develop in the inertial range of the spectrum. In the theory of thick reaction zones, cascade mechanisms are also introduced through both the fractal theory and a spectral analysis. In the inertial range the transfer of energy from scale L to smaller scales is due to advection by the turbulent motion. Thermal mixing may be supposed to depend on the same process in the whole range where molecular phenomena are not active. Starting from the similarity laws available in the domain where the viscosity effects may be neglected, multifractal theory uses the same point of view. Finally, the behaviour of volumes or surfaces is considered. The fractal concept may be used either as an introduction to intermittence or to an analysis of

surfaces embedded in flows. As far as the reactive zones can be identified with an immersed surface, it is easy to grasp the role played by fractal theory in the behaviour of the reactive zone. The domain of applicability of the method developed in this paper depends on the degree of universality of the fractal dimension. This is still an open question but we can presume that the presence of a wall implies specific adjustments.

A detailed analysis of the wall region should become easier. Starting from fractal theory, kinematic and chemical mechanisms could be tackled independently of each other.

REFERENCES

1. C. Dopazo, Recent development in P.D.F. methods. In *Turbulent Reacting Flows II* (Edited by Libby and Williams), Chap. 7. Springer-Verlag, Berlin.
2. F. A. Williams, The role of theory in combustion science, 24*th Symposium* (*International*) *on Combustion*, pp. 1–17 (1992).
3. J. Mathieu, D. Escudié and M. Lance, Premixed turbulent flames and spectral approach, *Rev. l'Institut Français du Pétrole* **44,** 519–546 (1989).
4. M. Barrère, Modèles de combustion turbulente, *Rev. Générale de Thermique* **148,** 295 (1974).
5. L. Delamare, R. Borghi and M. Gonzalez, The modelling and calculation of a turbulent premixed flame propagation in a closed vessel: comparisons of three models with experiments, SAE paper 910265 (March 1991).
6. N. Peters, Laminar flamelet concepts in turbulent combustion, *Twenty-first Symposium* (*International*) *on Combustion*, The Combustion Institute, Pittsburgh, pp. 1231–1250 (1986).
7. T. Poinsot, D. Veynante and S. M. Candel, Quenching processes and premixed turbulent combustion diagrams, *J. Fluid Mech.* **228,** 561–606 (1991).
8. T. Poinsot, D. Veynante and S. M. Candel, Diagram of premixed turbulent combustion based on direct simulation, 23*rd Symposium* (*International*) *on Combustion*, The Combustion Institute, Pittsburgh, pp. 613–619 (1990).
9. N. Darabiha, V. Giovangigli, A. Trouvé, S. M. Candel and E. Esposito, Coherent flame description of turbulent premixed ducted flames. In *Turbulent Reactive Flows* (Edited by R. Borghi and S. N. B. Murthy), pp. 591–637. Springer-Verlag, New York (1989).
10. E. Maistret, N. Darabiha, T. Poinsot, D. Veynante, F. Lacas, S. Candel and E. Esposito, Recent developments in the coherent flamelet description of turbulent combustion. In *Numerical Combustion* (Edited by A. Dervieux and B. Larrouturou), pp. 98–117. Springer-Verlag, Berlin (1989).
11. S. Candel, D. Veynante, F. Lacas, E. Maistret, N. Darabiha and T. Poinsot, Coherent flamelet model: applications and recent extensions. In *Advances in Combustion Modeling* (Edited by B. Larrouturou), pp. 19–64 (Series on Advances in Math. for Appl. Sci.). World Scientific, Singapore (1991).
12. F. C. Gouldin, Interpretation of jet mixing using fractals, *AIAA J.* **26,** 1405–1407 (1988).
13. J. Mantzaras, P. G. Felton and F. V. Bracco, Three-dimensional visualization of premixed-charge engine flame: islands of reactants and products; fractal dimensions; and homogeneity, SAE paper 881635 (1988).
14. D. A. Santavicca, D. Liou and G. North, A fractal model of turbulent flame kernel growth, SAE paper 900024 (1990).
15. R. Borghi, On the structure and morphology of turbulent premixed flames. In *Recent Advances in the Aerospace Sciences* (Edited by C. Casci) (1985).
16. F. C. Gouldin, K. N. C. Bray and J.-Y. Chen, Chemical closure model for fractal flamelets, *Combust. Flame* **77,** 241–225 (1989).
17. F. C. Gouldin, An application of fractals to modelling premixed turbulent flames, *Combust. Flame* **68,** 249–266 (1987).
18. C. Meneveau and T. Poinsot, Stretching and quenching of flamelets in premixed turbulent combustion, *Combust. Flame* **86,** 311–333 (1991).
19. K. R. Sreenivasan and C. Meneveau, The fractal facets of turbulence, *J. Fluid Mech.* **173,** 357–386 (1986).
20. K. R. Sreenivasan, R. Ramshankar and C. Meneveau, Mixing, entrainment and fractal dimensions of surfaces in turbulent flows, *Proc. R. Soc. Lond. A* **421,** 79–108 (1989).
21. C. Meneveau and K. R. Sreenivasan, Interface dimension in intermittent turbulence, *Phys. Rev. A* **41,** 2246–2248 (1990).
22. C. Meneveau, Analysis of turbulence in the orthonormal wavelet representation, *J. Fluid Mech.* **232,** 469–520 (1991).
23. Y. Gagne, Etude expérimentale de l'intermittence et des singularités dans le plan complexe en turbulence développée, Thèse de doctorat, Grenoble (1987).
24. J. C. Vassilicos and J. C. R. Hunt, Fractal dimensions and spectra of interfaces with application to turbulence, *Proc. R. Soc. Lond. A* **435,** 505–534 (1991).
25. F. Nicolleau and J. Mathieu, La notion de surface fractale et les modèles de prédiction, *Rev. Scientifique de la Défense* 95–102 (1992).
26. F. Nicolleau, J. P. Bertoglio and J. Mathieu, A contribution to turbulent combustion premixed flames and material surfaces, *Rev. l'Institut Français du Pétrole* **46**(1) (1991).
27. K. Kuo, *Principles of Combustion*, pp. 289–298. Wiley–Interscience, New York (1986).
28. F. A. Williams, *Combustion Theory*, pp. 135–145. Addison–Wesley, Reading, MA (1988).
29. F. Fichot, F. Lacas, D. Veynante and S. M. Candel, One-dimensional propagation of a premixed turbulence flame with a balance equation for the flame surface density, *Combust. Sci. Technol.* **90,** 35 (1993).
30. G. Z. Damköhler, Electrochemie Angewandte, *Phys. Chemie* 46601 (1940) [English translation, NACA T. M. 1112 (1947)].
31. J. P. Dumont, D. Durox and R. Borghi, Experimental study of the mean reaction rates in a turbulent premixed flame, *Combust. Sci. Technol.* **89,** 219–251 (1993).
32. D. Bradley, How fast can we burn?, 24*th Symposium* (*International*) *on Combustion*, pp. 247–262 (1992).
33. K. N. C. Bray, Studies of the turbulent burning velocity, *Proc. R. Soc. Lond. A* **431,** 315–335 (1990).
34. V. R. Kuznetsov and V. A. Sabel'nikov, *Turbulence and Combustion* (Edited by P. A. Libby), p. 237. Hemisphere Publishing Corporation.
35. G. Brun, Dévelopement et application d'une méthode d'éléments finis pourle calcul des écoulements turbulents fortement chauffés, Thèse de Doctorat, Ecole Centrale de Lyon, Ecully, France (1988).
36. M. Buffat, Simulation of two and three-dimensional internal subsonic flows using a finite element method, *Int. J. Numer. Meth. Fluids* **12,** (1991).
37. D. Bradley, A. K. C. Lau and M. L. Awes, Flame stretch rate as a determinant of turbulent burning velocity, *Phil. Trans. R. Soc. Lond. A* **338,** 359–387 (1992).
38. Y.-W. Chin, R. D. Matthew, S. P. Nichols and T. M. Kiehne, Use of fractal geometry to model combustion in SI engines, *Combust. Sci. Technol.* **86,** 1–30 (1992).